

Comparative analysis of quantum information measures of the Dirichlet and Neumann circular wells

O. Olendski

Department of Applied Physics and Astronomy, University of Sharjah, P.O. Box 27272, Sharjah, United Arab Emirates

Abstract

Derivation of the analytic expressions of the position and momentum wave functions of the Dirichlet and Neumann circular quantum wells allows an efficient calculation of the corresponding quantum information measures, such as Shannon entropy S , Fisher information I and Onicescu energy O for arbitrary principal n and magnetic m quantum numbers. A comparative analysis between the two types of the boundary conditions demonstrates the decreasing difference between the measures for the larger indexes what is explained by the lesser sensitivity of the higher-energy quantum states to the interface requirement. Mathematical results for S , I and O are explained from physical point of view; for instance, unrestricted decrease (increase) at $|m|$ or n tending to infinity of the position component of the entropy (Onicescu energy) is due to the transition from the quantum regime to the quasi-classical description. On the example of the lowest-energy Neumann orbital, it is demonstrated that i) the radial linear momentum operator is not a self-adjoint one and ii) two-dimensional entropic uncertainty relation is stronger than its Heisenberg counterpart.

Keywords: circular well, Shannon information entropy, Fisher information, Onicescu energy, boundary conditions

1. Introduction

Quantum structures with non Dirichlet boundary conditions (BCs) on the position wave function $\Psi(\mathbf{R})$, generally, do not obey Heisenberg uncertainty relation [1–4]. For instance, the latter is violated for the Neumann BC when the derivative of Ψ in the direction \mathbf{n} normal to the confining interface \mathcal{S} turns to zero:

$$\left. \frac{\partial \Psi}{\partial \mathbf{n}} \right|_{\mathcal{S}} = 0. \quad (1)$$

Email address: oolendski@sharjah.ac.ae (O. Olendski)

An example which can be called a canonical one [1–3] considers a one-dimensional (1D) quantum well extending along the X axis from $-d/2$ to $d/2$ with the position waveform satisfying

$$\Psi'(-d/2) = \Psi'(d/2) = 0. \quad (2)$$

Then, the lowest energy of this geometry and the corresponding function that are eigen solutions of the 1D version of the general l D (l is a positive integer) Schrödinger equation

$$-\frac{\hbar^2}{2M}\nabla_{\mathbf{R}}^2\Psi(\mathbf{R}) + V(\mathbf{R})\Psi(\mathbf{R}) = E\Psi(\mathbf{R}), \quad (3)$$

where $V(\mathbf{R})$ is an external potential in which an electrically charged particle with mass M is moving, are zero and constant $\Psi_0^N(X) = d^{-1/2}$, respectively. Note that the waveform obeys a normalization condition:

$$\int_{\mathbb{R}^l} \Psi^2(\mathbf{R})d\mathbf{R} = 1. \quad (4)$$

1D Heisenberg uncertainty relation is written as:

$$\Delta X \Delta K \geq \frac{1}{2}, \quad (5)$$

where ΔX and ΔK are, respectively, position and wave vector standard deviations:

$$\Delta X = \sqrt{\langle X^2 \rangle - \langle X \rangle^2} \quad (6a)$$

$$\Delta K = \sqrt{\langle K^2 \rangle - \langle K \rangle^2}, \quad (6b)$$

where the associated moments $\langle X^n \rangle$ and $\langle K^n \rangle$, $n = 1, 2, \dots$, are expressed through the corresponding position $\Psi(X)$ and momentum $\Phi(K)$ wave functions:

$$\langle X^n \rangle = \int_{-d/2}^{d/2} X^n \rho(X) dX \quad (7a)$$

$$\langle K^n \rangle = \int_{-\infty}^{\infty} K^n \gamma(K) dK \quad (7b)$$

with the densities that in general are written as

$$\rho(\mathbf{R}) = |\Psi(\mathbf{R})|^2 \quad (8a)$$

$$\gamma(\mathbf{K}) = |\Phi(\mathbf{K})|^2. \quad (8b)$$

Wave vector function is a Fourier transform of its position counterpart:

$$\Phi(\mathbf{K}) = \frac{1}{(2\pi)^{l/2}} \int_{\mathbb{R}^l} e^{-i\mathbf{K}\mathbf{R}} \Psi(\mathbf{R}) d\mathbf{R}. \quad (9)$$

It obeys a very similar normalization condition:

$$\int_{\mathbb{R}^l} |\Phi(\mathbf{K})|^2 d\mathbf{K} = 1. \quad (10)$$

For the 1D Neumann ground level it is:

$$\Phi_0^N(K) = \left(\frac{2}{\pi d}\right)^{1/2} \frac{1}{K} \sin \frac{Kd}{2}, \quad (11)$$

from which it is elementary to show that Eq. (10) is indeed satisfied. However, second order moment $\langle K^2 \rangle$ and, accordingly, wave vector standard deviation ΔK diverge what makes the Heisenberg relation, Eq. (5), meaningless since it does not bring about any estimation on the bound of the product $\Delta X \Delta K$. If, instead of using the wave vector function $\Phi_0(K)$, one tries for finding ΔK to work in the position space using the operator $\hat{K} = -i\frac{d}{dX}$ acting upon the function $\Psi_0(X)$, the result is even more dramatic since it immediately yields $\Delta K = 0$ what means a violation of the uncertainty relation. As a result, the quantum information measures ΔX and ΔK can not serve as universal estimators applicable to the analysis of the quantum motion for the arbitrary system. Such role is played by the position S_ρ and momentum S_γ Shannon quantum information entropies:

$$S_\rho = - \int_{\mathbb{R}^l} \rho(\mathbf{R}) \ln \rho(\mathbf{R}) d\mathbf{R} \quad (12a)$$

$$S_\gamma = - \int_{\mathbb{R}^l} \gamma(\mathbf{K}) \ln \gamma(\mathbf{K}) d\mathbf{K}, \quad (12b)$$

which, as was rigorously proved by W. Beckner [5] and I. Białynicki-Birula and J. Mycielski [6] (BBM), for the l -dimensional particle satisfy the inequality

$$S_\rho + S_\gamma \geq l(1 + \ln \pi), \quad (13)$$

which presents a stronger bound on simultaneous measurement of the position and momentum than the Heisenberg uncertainty relation [7, 8]. Before calculating the entropies and convincing ourself that they really do obey the BBM relation, Eq. (13), let us point out to the fact that is very frequently disregarded or not properly addressed what might lead to obvious errors, as is shown in Secs. 2 and 3; namely, the entropies from Eqs. (12) were generalized for the continuous probability distributions from their discrete counterpart $S = -\sum_{n=1}^N p_n \ln p_n$ for the N distinct events with the probabilities p_n such that $\sum_{n=1}^N p_n = 1$ [9]. Accordingly, the discrete Shannon entropy is a dimensionless quantity whereas S_ρ and S_γ are measured, respectively, in positive and negative units of l times the logarithm of the distance, what is physically ambiguous. However, if one chooses some characteristic length of the system L [10] (for our example it is, of course, the well width d), one needs to treat as a spatial coordinate the dimensionless quantity

$$\mathbf{r} = \mathbf{R}/L \quad (14a)$$

and since the corresponding scale of the wave vector is $1/L$, the dimensionless unit for measuring it becomes

$$\mathbf{k} = \mathbf{K}L. \quad (14b)$$

As a result, position (momentum) Shannon entropy will be represented as a sum of two items where the first one is positive (negative) $\ln L^l$ and the second one is the dimensionless scaling-independent integral. Accordingly, the sum of S_ρ and S_γ is a dimensionless scaling- and width-independent quantity. Let us show this on the example of the lowest level of the Neumann QW. One has:

$$S_{\rho_0}^N = \ln d \quad (15a)$$

$$S_{\gamma_0}^N = -\ln d - \frac{2}{\pi} \int_{-\infty}^{+\infty} \left(\frac{1}{k} \sin \frac{k}{2} \right)^2 \ln \left(\frac{2}{\pi} \frac{1}{k^2} \sin^2 \frac{k}{2} \right) dk \quad (15b)$$

and, accordingly,

$$S_{\rho_0}^N + S_{\gamma_0}^N = -\frac{2}{\pi} \int_{-\infty}^{+\infty} \left(\frac{1}{k} \sin \frac{k}{2} \right)^2 \ln \left(\frac{2}{\pi} \frac{1}{k^2} \sin^2 \frac{k}{2} \right) dk. \quad (15c)$$

Due to the simplicity of the system, the second term in the right-hand side of Eq. (15a) is missing; so, if we measure distances in units of the well width d , this Shannon entropy turns to zero [3]. The integral can be evaluated numerically yielding for the sum of the two entropies which we will denote by S_t the value of 2.6834 [3] satisfying, of course, inequality from Eq. (13) since $1 + \ln \pi = 2.1447$.

This example underlines a significance of studying Shannon entropies, especially for non-Dirichlet structures. Switching to the analysis of the 1D non-Cartesian geometries, a situation with the uncertainty relation gets even more weird. In fact, the very definition and meaning of the radial linear momentum operator \hat{P}_R in this case still remains a matter of controversy; namely, starting from the classical radial momentum $R^{-1}\mathbf{R} \cdot \mathbf{P}$, one symmetrizes it

$$\frac{1}{2} [R^{-1}\mathbf{R} \cdot \mathbf{P} + \mathbf{P} \cdot (R^{-1}\mathbf{R})] \quad (16)$$

and after the quantization the expression reads:

$$\hat{P}_R = -i\hbar \left(\frac{\partial}{\partial R} + \frac{l-1}{2} \frac{1}{R} \right). \quad (17)$$

Note that it obeys a correct commutation relation with the absolute value of the radius-vector R :

$$[R, \hat{P}_R] = i\hbar. \quad (18)$$

For $l = 3$, P.A.M. Dirac claims that " \hat{P}_R is real and is a true momentum conjugate to" R [11]. However, R.H. Dicke and J.P. Wittke retort that " \hat{P}_R is not the R -component of the particle momentum" [12] with A. Messiah adding that

\widehat{P}_R "is Hermitian but is not an observable" [13] since its eigenvalue problem, according to him, has no solution. Several authors tried to prove that \widehat{P}_R is not Hermitian [14–17]. In addition to the just mentioned sources, we refer the reader to Refs. [18–21] where more info on the subject is provided including historic references dating back to the early days of the wave mechanics. Considering quite dubious status of the operator \widehat{P}_R and, accordingly, of the product $\Delta R \Delta P$, the role of studying of the alternative to ΔR and ΔP quantum information measures in curvilinear multidimensional geometries increases many times higher.

In the present research, an exact analysis of the position and momentum components of the three quantum information measures is provided for the circle, $l = 2$, whose circumference \mathcal{S} supports either Dirichlet, $\Psi|_{\mathcal{S}} = 0$, or Neumann, Eq. (1), BC. In addition to the Shannon entropies, Fisher informations [22, 23]

$$I_\rho = \int \frac{|\nabla_{\mathbf{R}} \rho(\mathbf{R})|^2}{\rho(\mathbf{R})} d\mathbf{R} \quad (19a)$$

$$I_\gamma = \int \frac{|\nabla_{\mathbf{K}} \gamma(\mathbf{K})|^2}{\gamma(\mathbf{K})} d\mathbf{K}, \quad (19b)$$

and Onicescu energies [24], or disequilibria,

$$O_\rho = \int \rho^2(\mathbf{R}) d\mathbf{R} \quad (20a)$$

$$O_\gamma = \int \gamma^2(\mathbf{K}) d\mathbf{K} \quad (20b)$$

are included into the consideration too where in Eqs. (19b) and (20b), to be consistent with the entropy, we switched back to the wave vectors according to $\mathbf{P} = \hbar \mathbf{K}$. Functionals from Eq. (12), (19) and (20) define different facets of quantum distribution inside the confining volume; namely, its spreading, its oscillation structure and departure from equilibrium, respectively [25]. Their general physical and mathematical properties and meaning are thoroughly described in many sources and we will use some of them while explaining the results obtained; so, right now let just point out that position Fisher information is measured in inverse square of the length what makes its wave vector counterpart to represent the area whereas Onicescu energies are counted in units of the inverse volume of the manifold in which they are being operated upon. It means that the products $I_\rho I_\gamma$ and $O_\rho O_\gamma$, similar to the sum $S_\rho + S_\gamma$, are universal scaling- and volume-independent dimensionless quantities what allows a direct comparison between the outcomes of calculations by the different groups. Contrary to the Shannon entropy with its fundamental inequality, Eq. (13), similar universal restrictions for the Fisher information or Onicescu energy are not known though some lower (for $I_\rho I_\gamma$ [26–30]) or upper (for $O_\rho O_\gamma$ [31]) bounds involving the products of position and wave vector components have been obtained for several particular systems. From these three, one can form combined

measures; for example, statistical complexity introduced by R. G. Catalán, J. Garay, and R. López-Ruiz [32]

$$CGL = e^S O, \quad (21)$$

which, as it follows from our discussion above, is a dimensionless quantity, describes not only the randomness (due to the contribution from the first term in it) but also a deviation from uniformity that is handled by the multiplier O . This quantum information measure stays invariant under scaling, translation and replication [32] and either its position or momentum component in any l -dimensional space can never be less than unity [33]

$$CGL \geq 1, \quad (22)$$

with the equality being reached only for the uniform distribution with a finite volume support. As is shown in Sec. 3, this is really a case for the lowest Neumann orbital when its position waveform is just the constant.

As a first step in our discussion, we derive an analytic expression for the position waveform $\Psi(\mathbf{R})$ that solves Eq. (3) and satisfies the corresponding type of the BC. In fact, these normalized solutions involving Bessel functions are well known, especially for the Dirichlet requirement. Next, utilizing their properties, *analytic* formulas for the wave vector dependencies $\Phi(\mathbf{K})$ are obtained what greatly facilitates an understanding of their structure and subsequent computation of the quantum information measures. A discussion of the derived expressions for the Shannon entropies naturally pushes to switch to the dimensionless units from Eqs. (14). Physical explanation of the obtained mathematical results is provided. In the limiting cases, analytic asymptotics of the measures are derived. It is shown that the radial linear momentum operator from Eq. (17) is not a Hermitian one when acting on the Neumann manifold. It is demonstrated that in the 2D Neumann case, the Heisenberg uncertainty relation is weaker than its entropic counterpart. We also compare our results for the Dirichlet Shannon entropies with the previous calculations [34, 35] and point out the latter's deficiencies and blunders.

2. Dirichlet Well

2.1. General Consideration

We consider a motion of the quantum particle with mass M inside a disc of the radius d . Then, the 2D Schrödinger equation for the position wave function $\Psi(\mathbf{R})$ in polar coordinates $(R, \varphi_{\mathbf{R}})$ reads:

$$-\frac{\hbar^2}{2M} \left[\frac{1}{R} \frac{\partial}{\partial R} \left(R \frac{\partial \Psi}{\partial R} \right) + \frac{1}{R^2} \frac{\partial^2 \Psi}{\partial \varphi_{\mathbf{R}}^2} \right] = E \Psi, \quad (23)$$

what, upon separation of variables

$$\Psi_{mn}(R, \varphi_{\mathbf{R}}) = \frac{1}{\sqrt{2\pi}} e^{im\varphi_{\mathbf{R}}} \mathcal{R}_{mn}(R), \quad (24)$$

expresses the radial part $\mathcal{R}_{mn}(R)$ in terms of the Bessel functions $J_m(x)$ [36]:

$$\mathcal{R}_{mn}(R) = N_{mn} J_{|m|} \left(\sqrt{\frac{2ME}{\hbar^2}} R \right) \quad (25)$$

with the constant N_{mn} guaranteeing that Ψ does satisfy the orthonormality condition:

$$\int \Psi_{m'n'}^*(\mathbf{R}) \Psi_{mn}(\mathbf{R}) d\mathbf{R} \equiv \int_0^{2\pi} d\varphi_{\mathbf{R}} \int_0^d dR R \Psi_{m'n'}^*(R, \varphi_{\mathbf{R}}) \Psi_{mn}(R, \varphi_{\mathbf{R}}) = \delta_{mm'} \delta_{nn'}, \quad (26)$$

$m, m' = 0, \pm 1, \pm 2, \dots$, $n, n' = 1, 2, \dots$, and $\delta_{nn'}$ is a Kronecker delta. Energy spectrum E_{mn} and, accordingly, waveforms Ψ_{mn} strongly depend on the type of the boundary condition (BC) at the circumference.

2.2. Wave functions

For the Dirichlet BC, the function vanishes at the confining rim,

$$\mathcal{R}(d) = 0,$$

and the energy spectrum turns to:

$$E_{mn}^D = \frac{\hbar^2 j_{|m|n}^2}{2Md^2}, \quad (27)$$

with $j_{\nu n}$ being n th root of the ν th order Bessel function [36], $J_{\nu}(j_{\nu n}) = 0$, whereas the associated waveform takes the form:

$$\Psi_{mn}^D(R, \varphi_{\mathbf{R}}) = \frac{1}{\pi^{1/2} d} \frac{J_{|m|}(j_{|m|n} r)}{J_{|m|+1}(j_{|m|n})} e^{im\varphi_{\mathbf{R}}}, \quad (28)$$

where, according to Eq. (14a), a dimensionless position

$$r = \frac{R}{d} \quad (29)$$

has been introduced that varies between zero and unity, $0 \leq r \leq 1$.

By general definition, 2D position $\Psi(\mathbf{R})$ and momentum $\Phi(\mathbf{K})$ wave functions are related as:

$$\Phi(\mathbf{K}) = \frac{1}{2\pi} \int e^{-i\mathbf{K}\mathbf{R}} \Psi(\mathbf{R}) d\mathbf{R}. \quad (30)$$

For our geometry, it yields:

$$\Phi_{mn}^D(p, \varphi_{\mathbf{P}}) = \frac{1}{2\pi} \frac{1}{\pi^{1/2} J_{|m|+1}(j_{|m|n})} \int_0^d dR R J_{|m|} \left(j_{|m|n} \frac{R}{d} \right) \int_0^{2\pi} d\varphi_{\mathbf{R}} e^{i[m\varphi_{\mathbf{R}} - KR \cos(\varphi_{\mathbf{R}} - \varphi_{\mathbf{K}})]}. \quad (31)$$

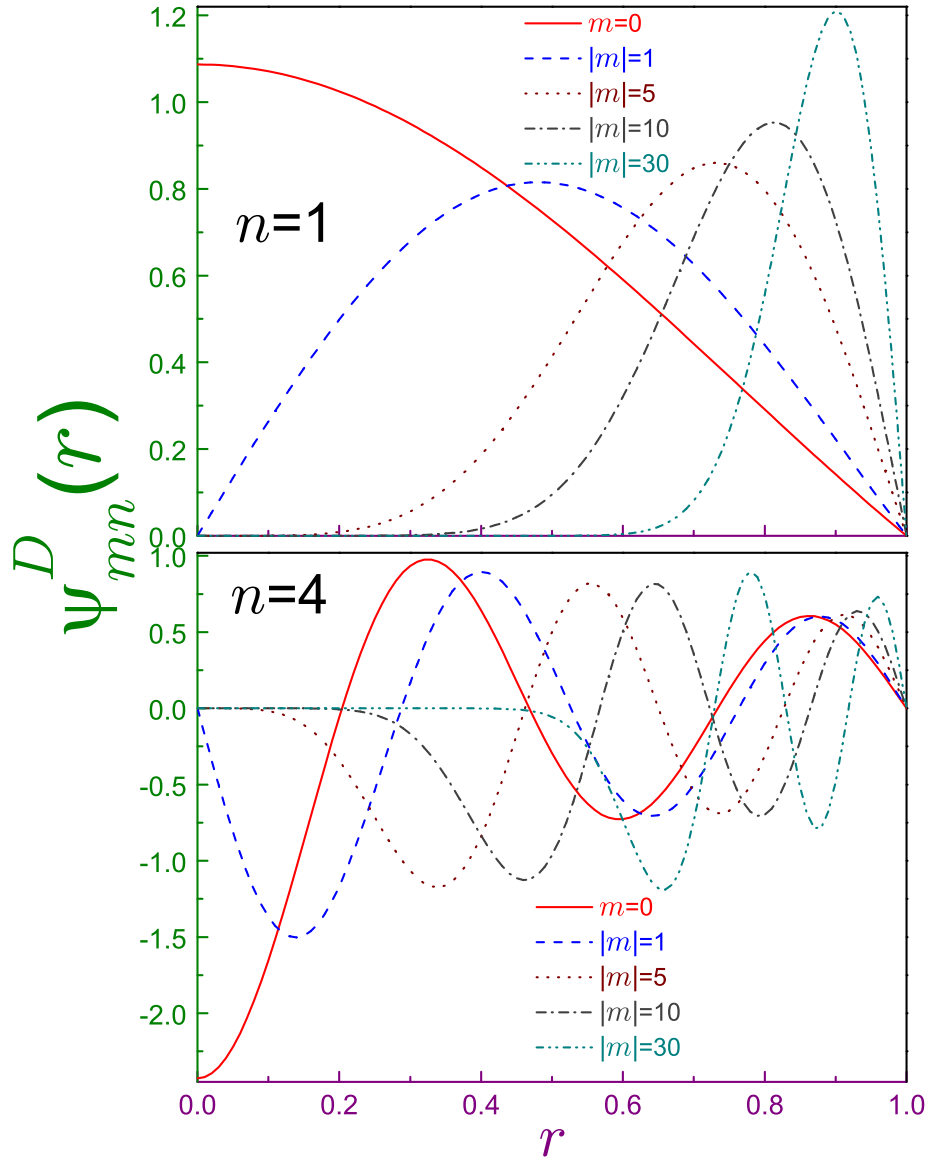


Figure 1: Functions $\psi_{mn}^D(r)$ from Eq. (39) for $n = 1$ (upper panel) and $n = 4$ (lower window) where solid lines are for $|m| = 0$, dash curves – for $|m| = 1$, dotted ones are for $|m| = 5$, dash-dotted lines – for $|m| = 10$, and dash-dot-dotted curves – for $|m| = 30$. Note different vertical scales in each of the subplots what is the case for all subsequent Figures too.

Polar integration in Eq. (31) is carried out with the help of the identity:

$$\int_0^{2\pi} e^{i[m\alpha - a \cos(\alpha - \beta)]} d\alpha = (-i)^m 2\pi J_m(a) e^{im\beta}. \quad (32)$$

By subsequent analytic evaluation of the radial quadrature with the help of known tables [37, 38], one arrives ultimately at

$$\Phi_{mn}^D(K, \varphi_{\mathbf{K}}) = d \frac{(-i)^m}{\pi^{1/2}} \frac{j_{|m|n}}{j_{|m|n}^2 - k^2} J_{|m|}(k) e^{im\varphi_{\mathbf{K}}}, \quad (33)$$

where the dimensionless wave vector k , according to Eq. (14b), is

$$k = Kd. \quad (34)$$

Obviously, orthonormalization of the position waveforms, Eq. (26), leads to the same property of their Fourier transforms:

$$\int \Phi_{m'n'}^*(\mathbf{K}) \Phi_{mn}(\mathbf{K}) d\mathbf{K} \equiv \int_0^{2\pi} d\varphi_{\mathbf{K}} \int_0^\infty dK K \Phi_{m'n'}^*(K, \varphi_{\mathbf{K}}) \Phi_{mn}(K, \varphi_{\mathbf{K}}) = \delta_{mm'} \delta_{nn'}, \quad (35)$$

what results in the following integral:

$$\int_0^\infty \frac{k}{(j_{|m|n}^2 - k^2)(j_{|m|n'}^2 - k^2)} J_{|m|}^2(k) dk = \frac{1}{2j_{|m|n}^2} \delta_{nn'}, \quad (36)$$

which is absent in known literature [36–40].

Thus, summing up this part of our research, we have shown that both position and momentum wave functions for the arbitrary principal n and magnetic m indexes can be represented *analytically* what was described in Ref. [34] as an impossible endeavor.

2.3. Quantum-information measures

A knowledge of the analytic representation of the position and momentum wave functions and, accordingly, of their associated densities

$$\rho_{mn}^D(\mathbf{R}) = \frac{1}{\pi d^2} \left[\frac{J_{|m|}(j_{|m|n} r)}{J_{|m|+1}(j_{|m|n})} \right]^2 \quad (37a)$$

$$\gamma_{mn}^D(\mathbf{K}) = \frac{d^2}{\pi} \left[\frac{j_{|m|n}}{j_{|m|n}^2 - k^2} J_{|m|}(k) \right]^2 \quad (37b)$$

paves the way to an efficient computation of all other characteristics of the Dirichlet well. In particular, Shannon entropies calculated from Eqs. (12) and

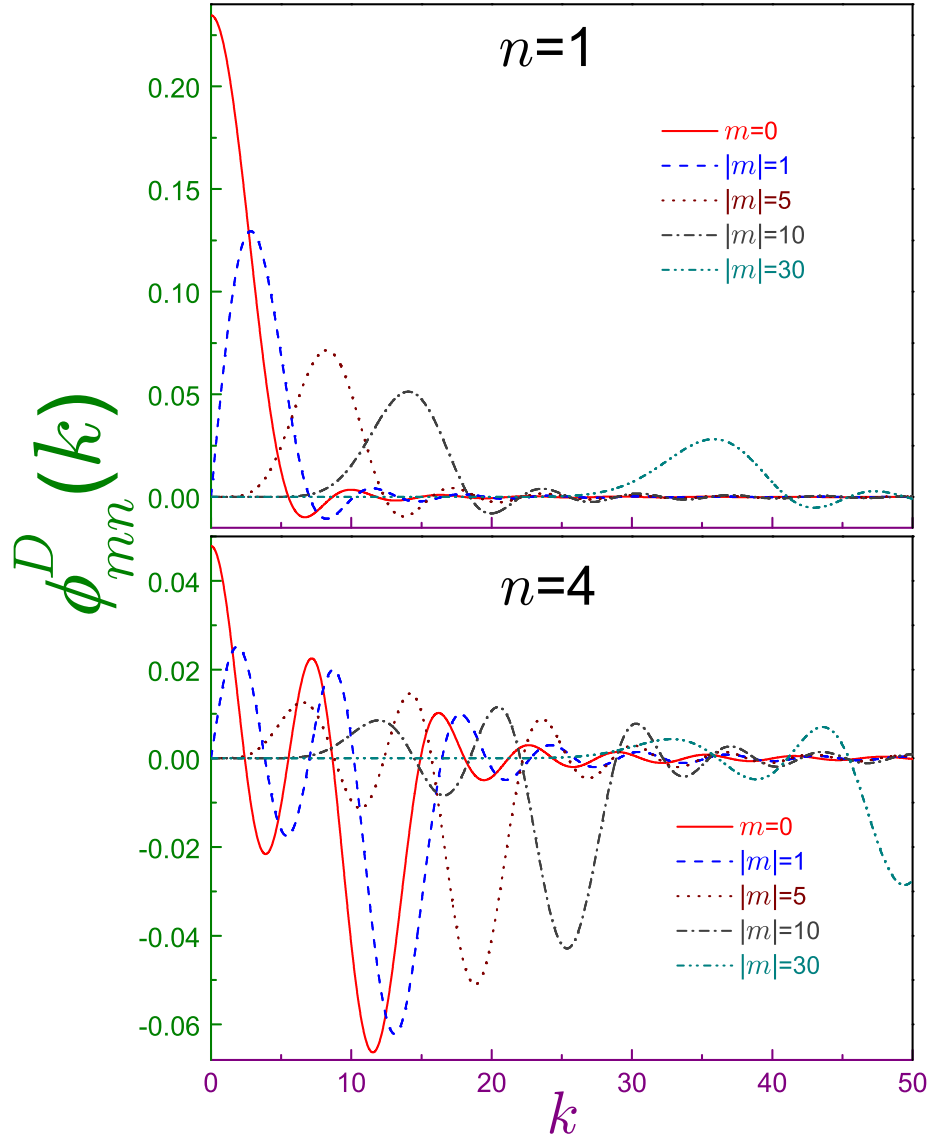


Figure 2: Functions $\phi_{mn}^D(k)$ from Eq. (40). The same convention as in Fig. 1 is adopted.

Table 1: Position $S_{\rho_{mn}}$ and momentum $S_{\gamma_{mn}}$ entropies together with their sum $S_{t_{mn}}$ for the Dirichlet disc

$ m $	Principal quantum number n											
	$n = 1$			$n = 2$			$n = 3$			$n = 4$		
	S_{ρ}^D	S_{γ}^D	S_t^D	S_{ρ}^D	S_{γ}^D	S_t^D	S_{ρ}^D	S_{γ}^D	S_t^D	S_{ρ}^D	S_{γ}^D	S_t^D
0	0.5942	3.8232	4.4174	0.5589	5.1255	5.6844	0.5488	5.7198	6.2686	0.5441	6.0988	6.6429
1	0.8103	4.6258	5.4361	0.6971	5.4655	6.1626	0.6494	5.9292	6.5786	0.6230	6.2487	6.8717
2	0.8215	5.0623	5.8838	0.7359	5.7100	6.4459	0.6888	6.0972	6.7860	0.6592	6.3760	7.0352
3	0.7934	5.3710	6.1644	0.7418	5.9050	6.6468	0.7037	6.2395	6.9432	0.6768	6.4878	7.1646
4	0.7547	5.6124	6.3671	0.7336	6.0685	6.8021	0.7063	6.3637	7.0700	0.6840	6.5879	7.2719
5	0.7136	5.8116	6.5252	0.7185	6.2100	6.9285	0.7019	6.4743	7.1762	0.6849	6.6788	7.3637
10	0.5252	6.4906	7.0158	0.6157	6.7300	7.3457	0.6419	6.9010	7.5429	0.6498	7.0420	7.6918
20	0.2560	7.2449	7.5009	0.4252	7.3605	7.7857	0.4986	7.4507	7.9493	0.5386	7.5320	8.0706
30	0.0685	7.7131	7.7816	0.2763	7.7725	8.0488	0.3753	7.8235	8.1988	0.4343	7.8743	8.3086

(37) read:

$$S_{\rho_{mn}}^D = 2 \ln d - 2 \int_0^1 r \left[\frac{J_{|m|}(j_{|m|n} r)}{J_{|m|+1}(j_{|m|n})} \right]^2 \ln \frac{J_{|m|}^2(j_{|m|n} r)}{\pi J_{|m|+1}^2(j_{|m|n})} dr \quad (38a)$$

$$S_{\gamma_{mn}}^D = -2 \ln d - 2 \int_0^\infty k \left[\frac{j_{|m|n}}{j_{|m|n}^2 - k^2} J_{|m|}(k) \right]^2 \ln \left(\frac{1}{\pi} \left[\frac{j_{|m|n}}{j_{|m|n}^2 - k^2} J_{|m|}(k) \right]^2 \right) dk. \quad (38b)$$

These equations manifest that the whole dependence on the radius of the well for both entropies is determined by positive or negative double logarithm of d , as expected from our discussion in the Introduction. Accordingly, it is absolutely unnecessary to specifically plot entropies dependence on the radius, as it was done in Figures 10 and 11 of Ref. [34]. Moreover, if the dependence of the position Shannon entropy in the above mentioned figures looks about logarithmic [though neither the explicit formula from Eq. (38a) nor any discussion on the shape of the curves is provided there], their momentum counterparts do not look logarithmically at all what means that the computation of the momentum entropies is wrong due to the incorrect form of the wave vector functions Φ . We will return to the reliability of the results presented in Ref. [34] later in our analysis. Next, the sum of the two entropies S_t is a dimensionless scaling-independent quantity [10] with the integrals in it calculated on the manifolds of dimensionless position and wave vector what makes the variables r from Eq. (29) and k , Eq. (34), most convenient and useful ones. Accordingly, from now on we will work in these units only and when talking about S_ρ and S_γ , we mean by them the corresponding second terms in the right-hand sides of Eqs. (38). If the need arises to find dimensional either position or momentum entropy, one simply adds to or subtracts from them $2 \ln d$. Also, since in these units the momentum and wave vector are the same, we will use either of these words to refer the variable k . Position and momentum Fisher informations will be scaled in d^{-2} and d^2 , respectively. The same statement is correct for the 2D Onicescu energies too. In addition, under such choice of scaling of the distance, momenta will be measured in \hbar/d and the most convenient unit to measure energies is $\pi^2 \hbar^2 / (2M d^2)$ what transforms Eq. (27) into

$$E_{mn}^D = \left(\frac{j_{|m|n}}{\pi} \right)^2. \quad (27a')$$

Then, it also does make sense to look at the waveforms Ψ and Φ in these dimensionless coordinates as they represent universal probability distributions without fixing them to any particular choice of the radius d . Fig. 1 depicts real functions

$$\psi_{mn}(r) = \Psi_{mn}(r, \varphi_{\mathbf{r}}) e^{-im\varphi_{\mathbf{r}}}, \quad (39)$$

which do not depend on the sign of m , for several values of the principal and magnetic quantum indexes. As expected, the states with the greater $|m|$ are

shifted further from the origin and thus, accumulate stronger at the outer edge with the absolute value of the nearest extremum increasing as the large magnetic number grows. For the higher n , the number of oscillations does increase what, due to the presence of the gradients in Eqs. (19) results in higher values of the position Fisher information, see Table 2. Fig. 2 shows several real momentum functions

$$\phi_{mn}(k) = i^m \Phi_{mn}(k, \varphi_{\mathbf{k}}) e^{-im\varphi_{\mathbf{k}}} \quad (40)$$

for the Dirichlet BC. It is seen that, in particular, the states with the larger magnetic index are shifted to the greater momenta k and, similar to the position component, a number of oscillations increases with n .

In Table 1, the values of the position $S_{\rho_{mn}}^D$ and momentum $S_{\gamma_{mn}}^D$ Shannon entropies together with their sum $S_{t_{mn}}^D$ are provided for m from 0 to 30 and $n = 1 - 4$. Since there are no in known literature analytic expressions for the corresponding integrals [36–40], a direct numerical quadrature was employed in computing them. Our results show that the momentum entropy for the one fixed quantum number (m or n) is a monotonically increasing function of the second index. Since the associated density $\gamma_{mn}^D(\mathbf{k})$ is always smaller than unity, $S_{\gamma_{mn}}^D$ is positive for any combination of $|m|$ and n . Its position counterpart exhibits at the fixed n a nonmonotonic dependence on $|m|$; namely, its initial growth at the small and moderate magnetic quantum number turns into the decent with the subsequent growth of $|m|$. For the fixed $|m|$, the position entropy generally decreases with the principal quantum index: for the small and moderate magnetic index this dependence is a monotonic one whereas for the higher $|m|$ values, a maximum of S_{ρ} is observed on the discrete n axis. We will return to the explanation of these two behaviors at the end of Section. The sum of the two entropies is an increasing function of both indexes. Of course, BBM inequality is always satisfied for this BC with the lowest level $m = 0$, $n = 1$ coming closest to saturating it with $S_{t_{01}}^D = 4.4174$ whereas $2(1 + \ln \pi) = 4.28946$. Note that our calculations for the sum of the two entropies are different from those provided in Ref. [34] where these values are larger; say, X.-D. Song, G.-H. Sun and S.-H. Dong [34] compute it for $m = 0$, $n = 1$ as 5.9277 after which there is a huge jump to 12.9820 for the first excited orbital followed by the maximum of 15.8823 at $n = 4$ with the subsequent decrease at the greater principal quantum numbers. Such irregular nonmonotonic behavior sheds a strong doubt on the validity of those computations.

Position Fisher informations

$$I_{\rho_{mn}}^D = 8 \frac{j_{|m|n}^2}{J_{|m|+1}^2(j_{|m|n})} \int_0^1 r J'_{|m|}(j_{|m|n} r)^2 dr \quad (41a)$$

can be calculated analytically as:

$$I_{\rho_{mn}}^D = 4j_{|m|n}^2 - \frac{4|m|}{J_{|m|+1}^2(j_{|m|n})} \left[1 - J_0^2(j_{|m|n}) - 2 \sum_{k=1}^{|m|-1} J_k^2(j_{|m|n}) \right]. \quad (41b)$$

Table 2: Position $I_{\rho mn}$ and momentum $I_{\gamma mn}$ Fisher informations together with their product for the Dirichlet disc

$ m\rangle$	Principal quantum number n											
	$n = 1$			$n = 2$			$n = 3$			$n = 4$		
	I_{ρ}^D	I_{γ}^D	$I_{\rho}^D I_{\gamma}^D$	I_{ρ}^D	I_{γ}^D	$I_{\rho}^D I_{\gamma}^D$	I_{ρ}^D	I_{γ}^D	$I_{\rho}^D I_{\gamma}^D$	I_{ρ}^D	I_{γ}^D	$I_{\rho}^D I_{\gamma}^D$
0	0.2313E+2	0.8722	0.2018E+2	0.1219E+3	1.2458	0.1518E+3	0.2995E+3	1.2977	0.3887E+3	0.5562E+3	1.3142	0.7309E+3
1	0.3807E+2	0.7884	0.3002E+2	0.1565E+3	1.1708	0.1832E+3	0.3538E+3	1.2560	0.4444E+3	0.6302E+3	1.2883	0.8119E+3
2	0.5337E+2	0.7267	0.3879E+2	0.1912E+3	1.1075	0.2118E+3	0.4083E+3	1.2148	0.4960E+3	0.7043E+3	1.2603	0.8876E+3
3	0.6912E+2	0.6782	0.4688E+2	0.2263E+3	1.0535	0.2384E+3	0.4629E+3	1.1759	0.5443E+3	0.7786E+3	1.2320	0.9592E+3
4	0.8533E+2	0.6387	0.5450E+2	0.2618E+3	1.0066	0.2635E+3	0.5178E+3	1.1397	0.5902E+3	0.8531E+3	1.2044	0.1027E+4
5	0.1020E+3	0.6055	0.6174E+2	0.2977E+3	0.9655	0.2874E+3	0.5731E+3	1.1062	0.6340E+3	0.9279E+3	1.1779	0.1093E+4
10	0.1910E+3	0.4934	0.9426E+2	0.4838E+3	0.8154	0.3945E+3	0.8559E+3	0.9712	0.8313E+3	0.1308E+4	1.0629	0.1390E+4
20	0.3928E+3	0.3798	0.1492E+3	0.8871E+3	0.6471	0.5741E+3	0.1454E+4	0.8001	0.1164E+4	0.2100E+4	0.9016	0.1893E+4
30	0.6189E+3	0.3183	0.1970E+3	0.1326E+4	0.5500	0.7291E+3	0.2093E+4	0.6931	0.1451E+4	0.2934E+4	0.7937	0.2329E+4

Table 3: Position $O_{\rho mn}$ and momentum $O_{\gamma mn}$ Onicescu energies together with their product for the Dirichlet disc

$ m $	Principal quantum number n											
	$n = 1$			$n = 2$			$n = 3$			$n = 4$		
	O_{ρ}^D	O_{γ}^D	$O_{\rho}^D O_{\gamma}^D$	O_{ρ}^D	O_{γ}^D	$O_{\rho}^D O_{\gamma}^D$	O_{ρ}^D	O_{γ}^D	$O_{\rho}^D O_{\gamma}^D$	O_{ρ}^D	O_{γ}^D	$O_{\rho}^D O_{\gamma}^D$
0	0.6679	0.2909E-1	0.1943E-1	0.8730	0.7242E-2	0.6322E-2	0.9821	0.4178E-2	0.4103E-2	1.0567	0.2969E-2	0.3137E-2
1	0.4939	0.1188E-1	0.5868E-2	0.6245	0.5263E-2	0.3287E-2	0.7092	0.3461E-2	0.2454E-2	0.7718	0.2596E-2	0.2004E-2
2	0.4871	0.7649E-2	0.3726E-2	0.5777	0.4197E-2	0.2424E-2	0.6449	0.2970E-2	0.1915E-2	0.6978	0.2312E-2	0.1613E-2
3	0.5023	0.5631E-2	0.2829E-2	0.5654	0.3497E-2	0.1977E-2	0.6192	0.2603E-2	0.1612E-2	0.6642	0.2085E-2	0.1384E-2
4	0.5237	0.4438E-2	0.2324E-2	0.5655	0.2996E-2	0.1694E-2	0.6086	0.2318E-2	0.1411E-2	0.6468	0.1898E-2	0.1228E-2
5	0.5471	0.3647E-2	0.1995E-2	0.5714	0.2619E-2	0.1496E-2	0.6055	0.2088E-2	0.1264E-2	0.6380	0.1742E-2	0.1111E-2
10	0.6661	0.1869E-2	0.1245E-2	0.6279	0.1588E-2	0.9970E-3	0.6299	0.1387E-2	0.8740E-3	0.6414	0.1231E-2	0.7893E-3
20	0.8784	0.8878E-3	0.7798E-3	0.7576	0.8582E-3	0.6502E-3	0.7191	0.8125E-3	0.5843E-3	0.7044	0.7639E-3	0.5381E-3
30	1.0633	0.5585E-3	0.5939E-3	0.8788	0.5724E-3	0.5030E-3	0.8106	0.5634E-3	0.4569E-3	0.7587	0.5255E-3	0.3986E-3

This expression looks much simpler than the one provided in Ref. [35]. Note that Figure 10 there plots I_ρ as a function of the well radius d . Similar to the Shannon entropy, there is no need in this since, as we discussed above, it is simply a d^{-2} dependence. Numerical results from Eq. (41b), together with their momentum counterparts, are given in Table 2 where also the products of the two informations are provided. Obviously, $I_{\rho mn}^D$ grows both with m and n whereas the momentum component is an increasing (decreasing) function of the principal (magnetic) index in such a way that the product $I_\rho I_\gamma$ gets greater for either of the quantum numbers enlarging. The decrease of the momentum component with $|m|$ growing can be understood from Figure 2 that shows a suppression of oscillations for the larger $|m|$ and since, due to the presence of the gradients in Eqs. (19), Fisher information is a local measure of distribution that is very sensitive to speed of change of the corresponding density, I_γ drops for the larger $|m|$.

The most characteristic features of the Onicescu energies presented in Table 3 are:

- both O_γ^D and $O_\rho^D O_\gamma^D$ decrease with $|m|$ and n growing;
- O_ρ^D is a concave function of the magnetic quantum number with its minimum (whose magnitude increases with n) being achieved at the larger $|m|$ for the greater principal index;
- for small and moderate $|m|$, the position disequilibrium monotonically increases with n ; however, for the greater magnetic index (for example, $|m| = 10$ and above) the Onicescu energy O_ρ^D has a minimum on the discrete n axis. This behavior is opposite to the one discussed for the Shannon entropy.

The first dependence can be understood by recalling that, physically, the Onicescu energy describes a deviation from the equilibrium or the most probable distribution, which is a uniform one. Figure 2 shows that for the larger $|m|$ the structure of the momentum waveforms gets more uniform thus decreasing I_γ . Second item is treated in a similar way; say, for $n = 1$ (upper panel in Figure 1) the wave function for $|m| = 1$ (dashed line) is much more uniform than its cylindrically symmetric counterpart (solid curve): the former one, which is almost symmetric with respect to $r = 1/2$, vanishes at the ends of the interval with its maximum being smaller than the extremum for $m = 0$ dependence that exhibits a continuous decrease. As a result, $O_{\rho 11} < O_{\rho 01}$. The unlimited increase of the position Onicescu energy (or unrestricted decrease of the Shannon entropy) at the large magnetic index is explained by the mentioned above accumulation of the density ρ near the outer edge: one sees that for $|m| \gg 1$ the function Ψ is almost zero along the r axis and only near the interface it has a sharp maximum which destroys the uniformity thus rising O_ρ or precipitously sinking S_ρ . In the

extreme limit of the magnetic index tending to infinity, one has:

$$\left\{ \begin{array}{c} \psi_{mn}(r) \\ \phi_{mn}(k) \\ S_{\rho mn} \\ S_{\gamma mn} \\ O_{\rho mn} \\ O_{\gamma mn} \end{array} \right\} \rightarrow \left\{ \begin{array}{c} \delta(r-1) \\ 0 \\ -\infty \\ \infty \\ \infty \\ 0 \end{array} \right\}, \quad |m| \rightarrow \infty. \quad (42)$$

Here, $\delta(z)$ is a Dirac δ -function. For example, the fading of the momentum waveform can be shown explicitly from its analytic representation, Eq. (33), and known asymptotic formula for the Bessel function with large index [36]:

$$J_\nu(z) \rightarrow \frac{1}{(2\pi\nu)^{1/2}} \left(\frac{ez}{2\nu}\right)^\nu, \quad \nu \rightarrow \infty. \quad (43)$$

Physically, Shannon entropy describes quantitatively the lack of our knowledge about the phenomenon; so, its extremely large negative (positive) values for the position (momentum) component manifest that we know precisely where the particle is located (know nothing about its momentum). The deviation of the position and momentum Shannon entropies in the opposite directions in this limit leads to the increase of their sum, as exemplified by Table 1. In general, the growth of the principal or magnetic quantum number means a shift to higher energies, as it follows from Eq. (27a') and properties of the zeros of Bessel functions [36]. Accordingly, with $|m|$ or n tending to infinity, one departs more and more from the quantum regime approaching the classical behavior when the position of the particle can be exactly specified what corresponds to the infinitely negative position entropy.

To save space, we do not provide a separate table for the complexity *CGL*. This can be easily done by compiling corresponding entries from Tables 1 and 3. Of course, the bound from Eq. (22) is always satisfied; in fact, for the Dirichlet well the complexity is always strictly greater than unity.

3. Neumann well

For this BC type, a normal derivative of the wave function vanishes at the interface:

$$\left. \frac{d}{dr} \mathcal{R}(r) \right|_{r=1} = 0.$$

Energy spectrum becomes:

$$E_{mn}^N = \left(\frac{j'_{|m|n}}{\pi} \right)^2, \quad (44)$$

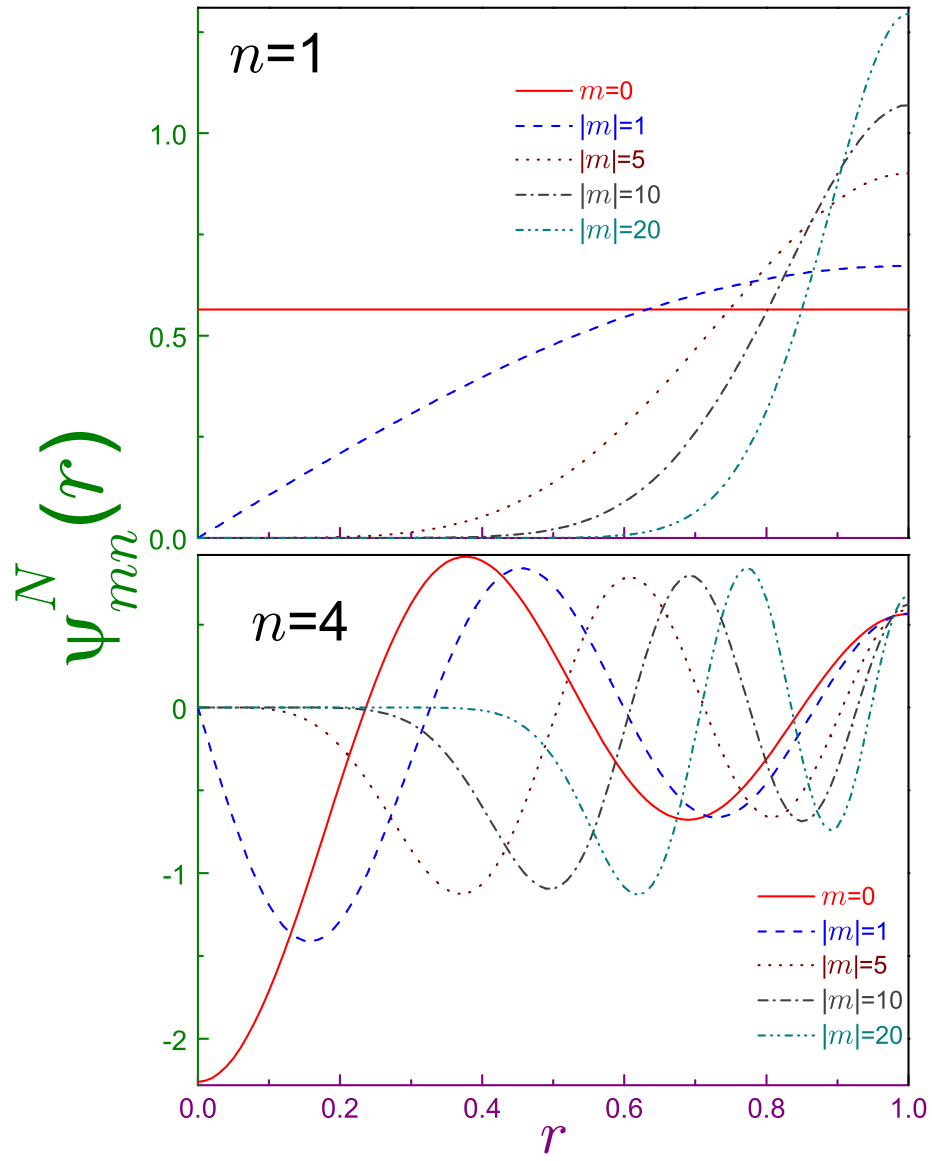


Figure 3: The same as in Fig. 1 but for the Neumann BC. Note also that dash-dot-dotted curves here are for $m = 20$.

where $j'_{\nu n}$ is the n th root of the derivative of the ν th order Bessel function [36], $J'_\nu(j'_{\nu n}) = 0$. Position waveforms read:

$$\Psi_{mn}^N(r, \varphi_{\mathbf{r}}) = \frac{1}{\pi^{1/2}} e^{im\varphi_{\mathbf{r}}} \begin{cases} 1, & m = 0, n = 1 \\ \frac{j'_{|m|n}}{(j'_{|m|n}{}^2 - m^2)^{1/2}} \frac{J_{|m|}(j'_{|m|n}r)}{J_{|m|}(j'_{|m|n})}, & \text{all other cases,} \end{cases} \quad (45)$$

and their momentum counterparts are:

$$\Phi_{mn}^N(\mathbf{k}) = \frac{(-i)^m}{\pi^{1/2}} e^{im\varphi_{\mathbf{k}}} \begin{cases} J_1(k)/k, & m = 0, n = 1 \\ \frac{j'_{|m|n}}{(j'_{|m|n}{}^2 - m^2)^{1/2}} \frac{k}{j'_{|m|n}{}^2 - k^2} J'_{|m|}(k), & \text{all other cases.} \end{cases} \quad (46)$$

Note that the functions $\Phi_{mn}^N(\mathbf{k})$ have in their denominators one k power less than their Dirichlet counterpart, see, e.g., Eq. (33), what will have a drastic consequence on calculating Δk below. Orthonormality from Eq. (35) yields:

$$\int_0^\infty \frac{k^3}{(j'_{|m|n}{}^2 - k^2)(j'_{|m|n'}{}^2 - k^2)} J'_{|m|}(k)^2 dk = \frac{1}{2} \left[1 - \left(\frac{m}{j'_{|m|n}} \right)^2 \right] \delta_{nn'}. \quad (47)$$

So, similar to the Dirichlet configuration, an analytic representation of the position and momentum wave functions is possible what again can be employed in the analysis of quantum-information measures. Corresponding dependencies $\psi_{mn}^N(r)$ and $\phi_{mn}^N(k)$ are shown in Figs. 3 and 4, respectively. As it was the case for the Dirichlet well, position density builds up at the interface with magnetic index growing what is accompanied by flattening the momentum component and subduing its oscillations.

The state with $m = 0$ and $n = 1$ deserves a special attention: its energy is zero (since $j'_{01} = 0$ [36]) and its position independent waveform is just $\pi^{-1/2}$. In addition, it is the only Neumann orbital that has a non vanishing probability of observing the zero momentum of the particle while for the Dirichlet BC it was true for any $m = 0$ level. It is elementary to calculate its position measures:

$$S_{\rho_{01}}^N = \ln \pi \quad (48a)$$

$$I_{\rho_{01}}^N = 0 \quad (48b)$$

$$O_{\rho_{01}}^N = 1/\pi \quad (48c)$$

together with

$$I_{\gamma_{01}}^N = 2. \quad (48d)$$

Eqs. (48a) and (48c) when substituted into Eq. (21) produce:

$$CGL_{\rho_{01}}^N = 1. \quad (48e)$$

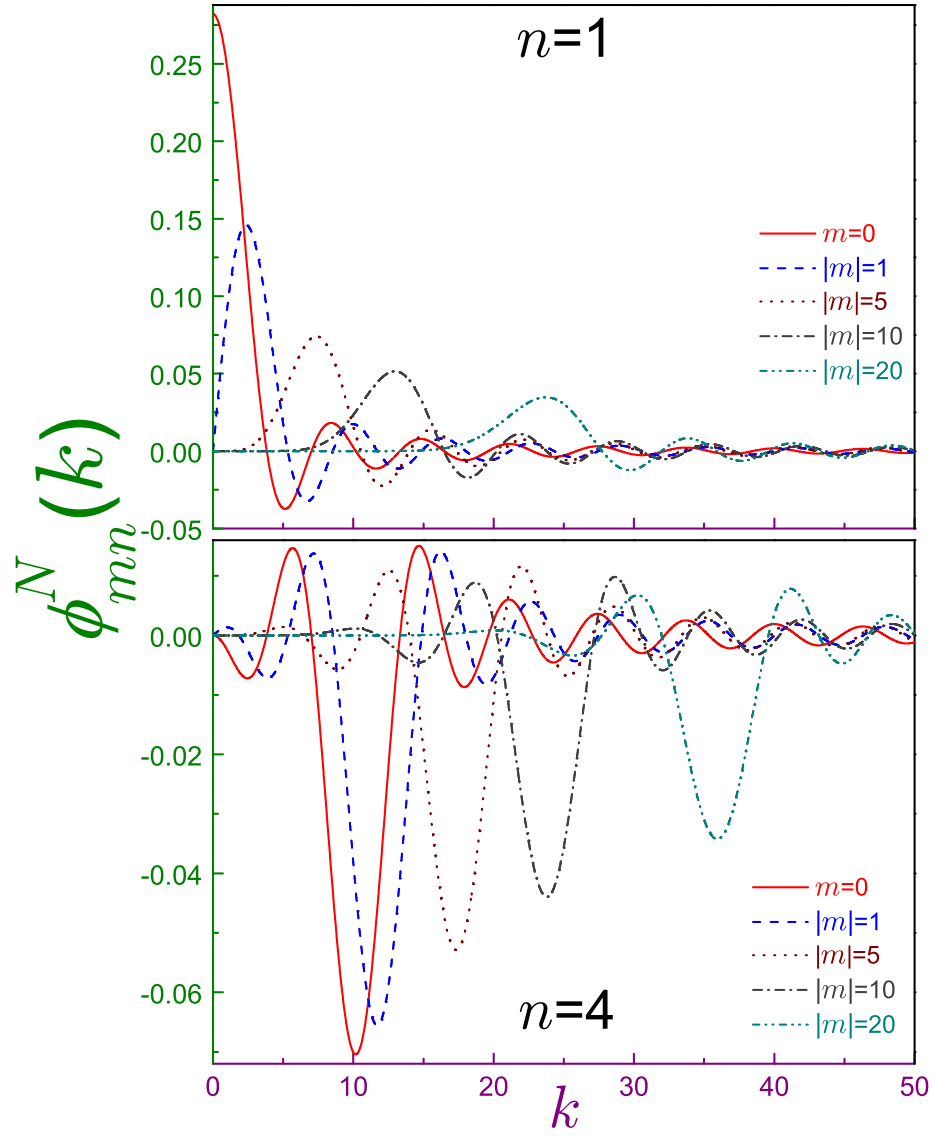


Figure 4: The same as in Fig. 2 but for the Neumann BC. The same convention as in Fig. 3 is adopted.

Table 4: Position $S_{\rho mn}$ and momentum $S_{\gamma mn}$ entropies together with their sum $S_{t mn}$ for the Neumann disc

$ m $	Principal quantum number n											
	$n = 1$			$n = 2$			$n = 3$			$n = 4$		
	S_{ρ}^N	S_{γ}^N	S_t^N	S_{ρ}^N	S_{γ}^N	S_t^N	S_{ρ}^N	S_{γ}^N	S_t^N	S_{ρ}^N	S_{γ}^N	S_t^N
0	1.1447	4.2880	5.4327	0.5647	5.3874	5.9521	0.5509	5.8924	6.4433	0.5452	6.2274	6.7726
1	1.0379	5.2247	6.2626	0.7411	5.6814	6.4225	0.6693	6.0761	6.7454	0.6344	6.3613	6.9957
2	0.9092	5.7280	6.6372	0.7724	5.9167	6.6891	0.7094	6.2344	6.9438	0.6725	6.4810	7.1535
3	0.7992	6.0786	6.8778	0.7659	6.1113	6.8772	0.7210	6.3724	7.0934	0.6891	6.5885	7.2776
4	0.7055	6.3489	7.0544	0.7456	6.2772	7.0228	0.7191	6.4949	7.2140	0.6944	6.6862	7.3806
5	0.6241	6.5702	7.1943	0.7199	6.4221	7.1420	0.7101	6.6053	7.3154	0.6930	6.7759	7.4689
10	0.3285	7.3085	7.6370	0.5806	6.9566	7.5372	0.6310	7.0355	7.6665	0.6465	7.1385	7.7850
20	-0.0203	8.1106	8.0903	0.3550	7.6054	7.9604	0.4659	7.5919	8.0578	0.5203	7.6318	8.1521

Thus, the general proof [33] about a saturation of the inequality from Eq. (22) is confirmed for the 2D case as the lowest-energy position waveform is just a constant on the finite interval, see solid line in the upper panel of Figure 3. Next, on the example of this orbital, let us show that in the 2D space the Heisenberg uncertainty relation that we will write in the form [41]

$$\Delta r \Delta k \geq 1, \quad (49)$$

similar to the 1D geometry, is weaker than its entropic counterpart, Eq. (13). In Eq. (49), Δr and Δk are, respectively, position and momentum standard deviations:

$$\Delta r = \sqrt{\langle r^2 \rangle - \langle r \rangle^2} \quad (50a)$$

$$\Delta k = \sqrt{\langle k^2 \rangle - \langle k \rangle^2}, \quad (50b)$$

with the position moments $\langle r^n \rangle$, $n = 1, 2, \dots$, being expressed through the corresponding densities:

$$\langle r^n \rangle = 2\pi \int_0^1 r^{n+1} \rho(r) dr, \quad (51a)$$

where, due to the polar symmetry, the argument of ρ has been replaced from the vector to its length. There are two options for calculating momentum powers $\langle k^n \rangle$: the first one uses, similar to $\langle r^n \rangle$, the associated density:

$$\langle k^n \rangle = 2\pi \int_0^\infty k^{n+1} \gamma(k) dk. \quad (51b)$$

Then, for any Neumann state including the $m = 0$, $n = 1$ level the momentum variance diverges and, accordingly, inequality (49) does not bring about any new information. Mathematically, the infinite value of $\langle k^2 \rangle$ for the Neumann geometry is due to the mentioned above property of the functions Φ whose convergence to zero at the large wave vector is slower than their Dirichlet counterparts. Second possibility applies the radial linear momentum operator from Eq. (17), which, in our dimensionless units we write here as

$$\widehat{k}_r = -i \left(\frac{\partial}{\partial r} + \frac{1}{2r} \right), \quad (17a')$$

and its square

$$\widehat{k}_r^2 = - \left(\frac{\partial^2}{\partial r^2} + \frac{1}{r} \frac{\partial}{\partial r} - \frac{1}{4r^2} \right), \quad (17a'')$$

to the function Ψ_{01}^N , which is just a constant. It is immediately seen that the operator \widehat{k}_r for this geometry is not a Hermitian one:

$$\left\langle \Psi_{01}^N \left| \widehat{k}_r \right| \Psi_{01}^N \right\rangle = -i. \quad (52)$$

Simultaneously, the matrix element $\langle \Psi_{01}^N | \hat{k}_r^2 | \Psi_{01}^N \rangle$ and, accordingly, the standard deviation Δk , logarithmically diverge. Thus, the use of the Heisenberg relation, Eq. (49), in either of its versions, for this configuration is senseless.¹ On the other hand, a corresponding entry in Table 4 manifests that the sum of the entropies for the lowest state does obey the BBM rule from Eq. (13), as expected. Neumann sum of 5.4327 is greater than its Dirichlet counterpart from Table 1. This rule holds true for any other level and is valid for the momentum components too. Position entropy of any state with $n \geq 2$ is, similar to the Dirichlet BC, a nonmonotonic function of the magnetic index whereas for $n = 1$ orbitals it steadily decreases with m and turns negative at $m = 20$ when $S_{\rho_{mn}}^D$ is still positive. Negative values of the position component mean that the parts of the function $|\psi_{20,1}^N(r)|$ from Eq. (39), which are greater than unity [and which, in the case of the lowest Neumann state, accumulate near the surface, see. Fig. 3(a)], overweigh in their contribution to the integral from Eq. (12a) those regions where $|\psi_{20,1}^N(r)| < 1$. For other principal quantum numbers, $n \geq 2$, this takes place at much greater magnetic indexes $|m|$ that, accordingly, are not shown in Tables 1 and 4. The difference between the Dirichlet and Neumann data decreases for the growing quantum numbers n and $|m|$ what is explained by the smaller sensitivity to the BC of the higher lying levels.

Table 5 that presents Fisher informations for the Neumann disc shows, in addition to the earlier obtained analytic results, Eqs. (48b) and (48d), a simple expression for the momentum components of the excited states with $m = 0$:

$$I_{\gamma_{0n}}^N = \frac{4}{3}, \quad n \geq 2. \quad (53)$$

All other features are qualitatively similar to those described in Sec. 2.3 for the Dirichlet well.

Finally, Onicescu energies for the Neumann BC are given in Table 6. Qualitatively, their properties are similar to their Dirichlet counterparts but quantitatively modified by the different type of the edge requirement; for example, position disequilibrium becomes a concave function of the principal index already at $|m| = 4$. As was the case with the other quantum information measures, the difference between the two types of the BCs diminishes for the larger indexes m and n . As a final observation, let us state that the limit of the extremely huge magnetic indexes from Eq. (42) remains true for the Neumann BC too.

4. Conclusions

Finding analytic form of the position and momentum wave functions allowed to efficiently calculate quantum-information measures of the Dirichlet and Neumann circular wells for arbitrary magnetic m and principal n quantum numbers

¹Note that for the Dirichlet orbitals the corresponding deviations stay finite and can be evaluated numerically as, for example, it was done in Ref. [35] by applying radial momentum operator, Eq. (17a'), and its square, Eq. (17a''), to the position functions from Eq. (28).

Table 5: Position $I_{\rho mn}$ and momentum $I_{\gamma mn}$ Fisher informations together with their product for the Neumann well

$ m\rangle$	Principal quantum number n											
	$n = 1$			$n = 2$			$n = 3$			$n = 4$		
	I_{ρ}^N	I_{γ}^N	$I_{\rho}^N I_{\gamma}^N$	I_{ρ}^N	I_{γ}^N	$I_{\rho}^N I_{\gamma}^N$	I_{ρ}^N	I_{γ}^N	$I_{\rho}^N I_{\gamma}^N$	I_{ρ}^N	I_{γ}^N	$I_{\rho}^N I_{\gamma}^N$
0	0	2	0	0.5873E+2	1.3333	0.7830E+2	0.1969E+3	1.3333	0.2625E+3	0.4140E+3	1.3333	0.5520E+3
1	4.1493	1.7629	7.3146	0.8338E+2	1.2950	0.1080E+3	0.2413E+3	1.3163	0.3176E+3	0.4782E+3	1.3240	0.6331E+3
2	8.7248	1.6200	0.1413E+2	0.1082E+3	1.2379	0.1339E+3	0.2858E+3	1.2842	0.3670E+3	0.5424E+3	1.3040	0.7073E+3
3	0.1370E+2	1.5180	0.2079E+2	0.1333E+3	1.1837	0.1578E+3	0.3305E+3	1.2487	0.4127E+3	0.6068E+3	1.2800	0.7766E+3
4	0.1901E+2	1.4393	0.2737E+2	0.1589E+3	1.1352	0.1804E+3	0.3756E+3	1.2135	0.4558E+3	0.6714E+3	1.2545	0.8423E+3
5	0.2463E+2	1.3754	0.3388E+2	0.1849E+3	1.0919	0.2019E+3	0.4211E+3	1.1799	0.4968E+3	0.7364E+3	1.2290	0.9050E+3
10	0.5634E+2	1.1698	0.6591E+2	0.3212E+3	0.9330	0.2997E+3	0.6547E+3	1.0411	0.6817E+3	0.1067E+4	1.1134	0.1188E+4
20	0.1328E+3	0.9692	0.1287E+3	0.6221E+3	0.7566	0.4707E+3	0.1154E+4	0.8640	0.9972E+3	0.1761E+4	0.9483	0.1670E+4

Table 6: Position $O_{\rho mn}$ and momentum $O_{\gamma mn}$ Onicescu energies together with their product for the Neumann disc

$ m\rangle$	Principal quantum number n											
	$n = 1$			$n = 2$			$n = 3$			$n = 4$		
	O_{ρ}^N	O_{γ}^N	$O_{\rho}^N O_{\gamma}^N$	O_{ρ}^N	O_{γ}^N	$O_{\rho}^N O_{\gamma}^N$	O_{ρ}^N	O_{γ}^N	$O_{\rho}^N O_{\gamma}^N$	O_{ρ}^N	O_{γ}^N	$O_{\rho}^N O_{\gamma}^N$
0	0.3183	0.3658E-1	0.1164E-1	0.8122	0.8427E-2	0.6844E-2	0.9429	0.4746E-2	0.4474E-2	1.0275	0.3296E-2	0.3387E-2
1	0.3718	0.1280E-1	0.4759E-2	0.5725	0.6057E-2	0.3468E-2	0.6735	0.3889E-2	0.2619E-2	0.7446	0.2859E-2	0.2129E-2
2	0.4356	0.7629E-2	0.3323E-2	0.5397	0.4709E-2	0.2541E-2	0.6155	0.3291E-2	0.2026E-2	0.6741	0.2523E-2	0.1701E-2
3	0.4946	0.5354E-2	0.2648E-2	0.5382	0.3840E-2	0.2067E-2	0.5953	0.2850E-2	0.1697E-2	0.6438	0.2257E-2	0.1453E-2
4	0.5492	0.4078E-2	0.2240E-2	0.5470	0.3233E-2	0.1768E-2	0.5893	0.2511E-2	0.1480E-2	0.6294	0.2041E-2	0.1284E-2
5	0.6006	0.3268E-2	0.1963E-2	0.5602	0.2785E-2	0.1560E-2	0.5901	0.2242E-2	0.1323E-2	0.6230	0.1862E-2	0.1160E-2
10	0.8238	0.1561E-2	0.1286E-2	0.6428	0.1614E-2	0.1037E-2	0.6289	0.1445E-2	0.9089E-3	0.6361	0.1286E-2	0.8181E-3
20	1.1846	0.7014E-3	0.8309E-3	0.8066	0.8373E-3	0.6754E-3	0.7364	0.8215E-3	0.6049E-3	0.7113	0.7801E-3	0.5549E-3

and to carry out a comparative analysis of the two types of the BC. As a result, the previous computations [34] of the Shannon entropies of the Dirichlet disc have been corrected and expanded to other density functionals, such as Fisher information and Onicescu energy. In particular, it was shown that the difference between the corresponding quantum information measures for the different surface requirements decreases at the higher indexes. It was demonstrated that the standard Heisenberg uncertainty relation for the lowest zero-energy Neumann orbital is meaningless and the radial linear momentum operator is not self-adjoint when applied to the 2D lowest-energy Neumann function. However, the fundamental inequality for the sum of the two entropies, Eq. (13), is satisfied by this state what is another manifestation of the fact that the BBM relation, Eq. (13), is stronger than its standard Heisenberg counterpart from Eq. (49).

5. Acknowledgments

Research was supported by SEED Project No. 1702143045-P from the Research Funding Department, Vice Chancellor for Research and Graduate Studies, University of Sharjah.

References

- [1] I. Białynicki-Birula, Ł. Rudnicki, in: *Statistical Complexity: Applications in Electronic Structure*, edited by K. D. Sen (Springer, Dordrecht, 2011), chap. 1.
- [2] M.H. Al-Hashimi, U.-J. Wiese, *Ann. Phys.* 327 (2012) 1.
- [3] O. Olendski, *Ann. Phys. (Berlin)* 527 (2015) 278.
- [4] O. Olendski, *Ann. Phys. (Berlin)* 528 (2016) 865.
- [5] W. Beckner, *Annals Math.* 102 (1975) 159.
- [6] I. Białynicki-Birula, J. Mycielski, *Commun. Math. Phys.* 44 (1975) 129.
- [7] S. Wehner, A. Winter, *New J. Phys.* 12 (2010) 025009.
- [8] P.J. Coles, M. Berta, M. Tomamichel, S. Wehner, *Rev. Mod. Phys.* 89 (2017) 015002.
- [9] C.E. Shannon, *Bell Syst. Tech. J.* 27 (1948) 379.
- [10] V.V. Dodonov, V.I. Man'ko, *Tr. Fiz. Inst. Akad. Nauk SSSR* 183 (1987) 5 [*Proc. Lebedev Phys. Inst. Acad. Sci. USSR* 183 (1989) 3].
- [11] P.A.M. Dirac, *The Principles of Quantum Mechanics* (Oxford, Clarendon, 1967).
- [12] R.H. Dicke and J.P. Wittke, *Introduction to Quantum Mechanics* (Reading, Massachusetts, Addison-Wesley, 1966).

- [13] A. Messiah, *Quantum Mechanics*, vol. 1 (Amsterdam, North-Holland, 1961).
- [14] R.L. Liboff, I. Nebenzahl, H.H. Fleischmann, *Am. J. Phys.* 41 (1973) 976.
- [15] O. Levin, A. Peres, *J. Phys. A* 27 (1994) L143.
- [16] J. Twamley, *J. Phys. A* 31 (1998) 4811.
- [17] G. Paz, *J. Phys. A* 35 (2002) 3727.
- [18] H. Essén, *Am. J. Phys.* 46 (1978) 983.
- [19] J.M. Domingos, M.H. Caldeira, *Found. Phys.* 14 (1984) 147.
- [20] G. Paz, *Eur. J. Phys.* 22 (2001) 337.
- [21] U. Roy, S. Ghosh, K. Bhattacharya, *Rev. Mex. Fis. E* 54 (2008) 160.
- [22] R.A. Fisher, *Math. Proc. Cambridge Philos. Soc.* 22 (1925) 700.
- [23] B.R. Frieden, *Science from Fisher Information* (Cambridge, Cambridge, 2004).
- [24] O. Onicescu, *C. R. Acad. Sci. Ser. A* 263 (1966) 841.
- [25] R.O. Esquivel, S. López-Rosa, M. Molina-Espíritu, J.C. Angulo, J.S. Dehesa, *Theor. Chem. Acc.* 135 (2016) 253.
- [26] A.J. Stam, *Inf. Control* 2 (1959) 101.
- [27] A. Dembo, T.M. Cover, J.A. Thomas, *IEEE Trans. Inf. Theory* 37 (1991) 1501.
- [28] E. Romera, P. Sánchez-Moreno, J.S. Dehesa, *Chem. Phys. Lett.* 414 (2005) 468.
- [29] J.S. Dehesa, A. Martínez-Finkelshtein, V.N. Sorokin, *Mol. Phys.* 104 (2006) 613.
- [30] J.S. Dehesa, R. González-Férez, P. Sánchez-Moreno, *J. Phys. A* 40 (2007) 1845.
- [31] A. Ghosal, N. Mukherjee, A.K. Roy, *Ann. Phys. (Berlin)* 528 (2016) 796.
- [32] R.G. Catalán, J. Garay, R. López-Ruiz, *Phys. Rev. E* 66 (2002) 011102.
- [33] S. López-Rosa, J.C. Angulo, J. Antolín, *Physica A* 388 (2009) 2081.
- [34] X.-D. Song, G.-H. Sun, S.-H. Dong, *Phys. Lett. A* 379 (2015) 1402.
- [35] A.J. Torres-Arenas, Q. Dong, G.-H. Sun, S.-H. Dong, *Phys. Lett. A* 382 (2018) 1752.

- [36] M. Abramowitz, I.A. Stegun (Eds.), Handbook of Mathematical Functions, Dover, New York, 1964.
- [37] I.S. Gradshteyn, I.M. Ryzhik, Tables of Integrals, Series, and Products, 7th ed., Academic Press, New York, 2014.
- [38] A.P. Prudnikov, Y.A. Brychkov, O.I. Marichev, Integrals and Series, vol. 2, Gordon and Breach, New York, 1992.
- [39] A.P. Prudnikov, Y.A. Brychkov, O.I. Marichev, Integrals and Series, vol. 3, Gordon and Breach, New York, 1992.
- [40] Y.A. Brychkov, Handbook of Special Functions, Taylor & Francis, Boca Raton, 2008.
- [41] C. Bracher, Am. J. Phys. 79 (2011) 313.